



Synthesis and microstructure studies of nano-sized cerium-zinc phosphates

Adly Abdella Hanna^a, Sahar Mohamed Mousa^a, Marwa Adel Sherief^{a,*} and Gehan Mahmoud Elkomy^b

^a Inorganic Chemistry Department, National Research Centre, Dokki, Cairo-11787, Egypt

^b Electron Microscopes and Thin Film Department, National Research Centre, Dokki, Cairo-11787, Egypt

*Corresponding author at: Inorganic Chemistry Department, National Research Centre, Dokki, Cairo-11787, Egypt. Tel.: +20.10.5249230; fax: +20.2.3335968. E-mail address: gohamora@yahoo.com (M.A. Sherief).

ARTICLE INFORMATION

Received: 20 April 2011

Received in revised form: 11 July 2011

Accepted: 22 July 2011

Online: 31 December 2011

KEYWORDS

Cerium phosphate

Zinc phosphate

Calcinations

X-ray diffraction

IR

TEM

ABSTRACT

A system of $\text{Ce}(\text{SO}_4)_2 \cdot 4\text{H}_2\text{O}$, $\text{Zn}(\text{CH}_3\text{COO})_2 \cdot 2\text{H}_2\text{O}$ and phosphoric acid was studied by the chemical reaction between the precursor materials. The cerium cations were replaced by zinc cations (x) in the range of $x = 0.0-1.0$. The obtained gels were dried and calcinated at 650 °C for 2 hrs. The effect of calcination on the produced phases was studied using X-ray diffraction (XRD) and infrared spectroscopy (IR). The thermal behaviors of only the dried samples were investigated employing differential scanning calorimetric (DSC) and thermogravimetric analysis (TGA). The transmission electron microscope (TEM) was used to investigate the morphology, crystallinity and particle size of both dried and calcined samples. The TEM results indicated that the crystallinity was improved by increasing the zinc contents. The importance of Zn, Ce phosphates return to their using as UV-shielding agents.

1. Introduction

Nowadays, the damaging effects of UV rays have been attracting attention because UV rays in sunlight causes many problems such as photo-degradation of organic materials and damages to human health e.g. causing sunburn, suntan, acceleration of aging, cancer, etc. [1-3]. Therefore, excellent sunscreen materials for UV shielding have been developed. The sunscreen products come in two basic forms: synthetic organic and inorganic compounds [4]. However, organic sunscreens may pose a safety problem when they are used at high concentrations, because some of organic UV absorbers cause irritation on the skin of sensitive individuals and demonstrative estrogenic activities [5,6]. Inorganic sunscreens, such as ultrafine titanium oxide, zinc oxide and cerium oxide, have been applied as effective sunscreens [7-9]. Titanium oxide and zinc oxide are popular inorganic sunscreen agents. However, the former is known as an excellent photocatalyst that may be harmful for the skin and sometimes affects other ingredients in the products. The latter has a photoinduced dissolution problem to form Zn^{2+} ions [10,11].

Although cerium oxide exhibits minimal photocatalysis, it has high catalytic activities for oxidation of organic compounds, as applied in oxidation, combustion and automotive exhaust cleaning catalysts [12]. So, the producing of inorganic compounds with excellent ultraviolet absorption ability and low side effect are needed. In recent years, considerable attention has been paid to the rare earth phosphates because of their potential applications for anti-UV materials [13-15].

Hanna *et al.* [16], prepared pure phases of cerium phosphate with monoclinic or hexagonal structure and studied the effects of various factors such as pH, precursor's materials and sintering temperatures on the morphology, crystallinity and particle size of the obtained product. In the present work, mixtures of cerium-zinc phosphates by substituting Ce^{3+}

cations with Zn^{2+} cations were prepared and the effect of substitution on the produced phases was studied. The morphology, thermal behavior, crystallinity and particle sizes of the produced phases were studied to draw some light on the using of their phosphates as UV-shielding agent in the future.

2. Experimental

2.1. Procedure

Cerium-zinc phosphates with different percentages of $\text{Zn}(x)$, ($x = 0.0, 0.2, 0.4, 0.6, 0.8$ and 1.0) were prepared by the co-precipitation method. Cerium sulfate tetrahydrate and zinc acetate dihydrate were dissolved in deionized water with continuous stirring at room temperature. Then, the required amount of H_3PO_4 was added dropwise. The pH of the final reaction was adjusted by ammonia to be alkaline ($\text{pH} \sim 8$). The stirring was continued for 1 hr. The formed precipitates were separated by centrifuging; then washed with deionized water and dried at 80 °C. An amount of each dried sample was calcined at 650 °C for 2 hrs. Table 1 summarized the amount of the reactant materials, which were used for cerium-zinc phosphates system.

Table 1. The amount of the reactant materials.

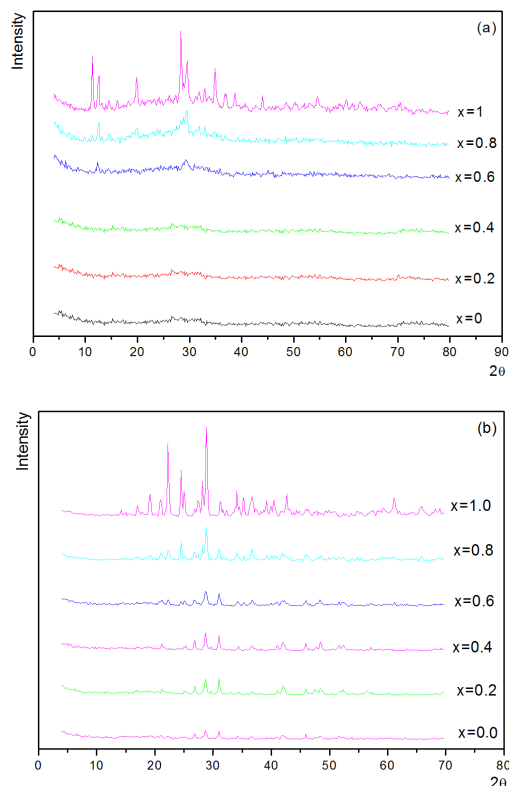
X value	$\text{Ce}(\text{SO}_4)_2 \cdot 4\text{H}_2\text{O}$ (g)	$\text{Zn}(\text{C}_4\text{H}_6\text{O}_4)_2 \cdot 2\text{H}_2\text{O}$ (g)	H_3PO_4 (mL)
0.0	5.0	0.0	0.84
0.2	4.0	1.63	1.00
0.4	3.0	3.26	1.18
0.6	2.0	4.89	1.35
0.8	1.0	6.52	1.51
1.0	0.0	8.15	1.68

2.2. Characterization

The structure and the phases of the produced samples were performed by X-ray diffraction where the diffraction patterns

Table 2. XRD results of calcinated Ce- Zn phosphates at 650 °C for 2 hr.

X value	Product phases	Chem. composition	Crys. structure
0.0-0.2	Monazite	CePO ₄	Monoclinic
0.4-0.8	Monazite	CePO ₄	Monoclinic
	Zinc pyrophosphate	Zn ₂ P ₂ O ₇	Orthorhombic
	Zinc phosphate	Zn ₃ (PO ₄) ₂	Monoclinic
1.0	Zinc pyrophosphate	Zn ₂ P ₂ O ₇	Orthorhombic
	Zinc phosphate	Zn ₃ (PO ₄) ₂	Monoclinic

**Figure 1.** X-ray diffraction patterns of as prepared and calcined cerium (a) and zinc (b) phosphate.

were obtained by using Bruker D8 advanced X-ray diffractometer with copper (K_{α}) radiation. Infrared measurements (IR) were recorded by JASCO-FT/CR-3000E infrared spectrophotometer in range from 4000 to 400 cm^{-1} and the thermal analysis was performed by USA Perkin-Elmer thermogravimetric up to 1000 °C with heating rate 10 °C/min. The morphology and the crystallinity of the produced samples before and after calcinations were examined by transmission electron microscope (TEM) Joel JEM 1230 working at 100 keV. Also Gatan program was used to calculate the d-spacing from the selected area electron diffraction SAED patterns.

3. Results and discussion

X-ray powder diffraction patterns show that the prepared samples with $x = 0.0-0.4$ are completely amorphous, while at $x = 0.6$ a weak crystalline phase becomes to appeared. For $x = 0.8$ and 1.0, the formed phases converted to well crystalline as shown in Figure 1. The analysis of the X-ray patterns indicates that the formed phases are CePO₄, ZnHPO₄ (35-574 card) and Zn₃(PO₄)₂·4H₂O(9-49 card) at $x = 0.8$. Only two new phases of ZnHPO₄ and Zn₃(PO₄)₂·4H₂O were formed at $x = 1.0$. By calcinating the samples at 650 °C for 2 hrs, only CePO₄ with monoclinic structure (Monazite) was formed at $x = 0.0$ or 0.2 (83-652). By the increase of zinc content to 0.4-1.0 a mixture of different phases was formed depending on the ratio between

Ce³⁺ and Zn²⁺. Table 2 represents the resulting phases. From X-ray results, it may be concluded that the substitution of Ce³⁺ by Zn²⁺ leads to improve the crystallinity of the produced samples. It seems that, the resulting CePO₄ with trivalent cations while it added in the tetravalent state, may be due to the reduction of Ce⁴⁺ to Ce³⁺ in the acidic medium (Cerium, Wikipedia, the free encyclopedia). This behavior may be resulting from the energy of the inner level 4f of the cerium is nearly the same as that of the outer valance electrons [17].

Figure 2 and 3 represents the IR spectrum of the as-prepared samples and that calcinated at 650 °C for 2 hrs. For the as-prepared samples an absorption band in the range from 3000 to 3900 cm^{-1} was observed. This band may be due to the stretching vibration of the OH groups which are attached with the moisture content or the phosphates groups, while the other band due to the H-O-H bending motion was observed in the region 1630-1650 cm^{-1} [18].

As observed frequently, the appearance of the absorption band for the phosphate compounds at 1400-1450 cm^{-1} was attributed to the carbonate group derived from the atmosphere during the preparation [19,20]. At $x = 0.0$, a series of bands are observed at 1067, 619 and 529 cm^{-1} corresponding to P-O stretching, O=P-O bending and O-P-O bending mode vibration respectively. The appearance of these bands is characteristic to the formation of hydrous CePO₄ as suggested previously by Hazal et al. [21].

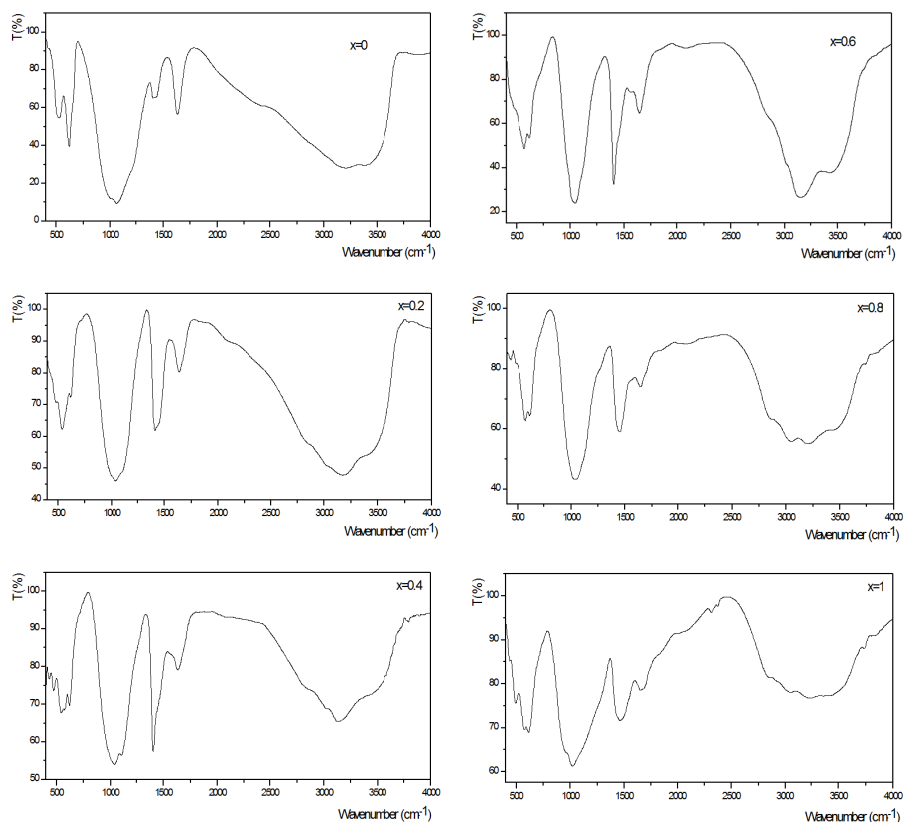


Figure 2. IR spectrum of as prepared and calcined samples of cerium phosphate.

For the spectrum of sample at $x = 0.2$, there are some shifts on the position of the bands which characterize hydrous CePO_4 ; these bands occurred at 1107, 617 and 536 cm^{-1} . Some additional bands occurred at 1036 and 473 cm^{-1} corresponding to anti-symmetric stretching mode of PO_4 group due to $\text{Zn}_3(\text{PO}_4)_2$ formation [22]. At $x = 0.4-1.0$, the IR spectra behaves nearly the same trend, with some shifts on the band position due to the substitution of Ce by Zn and formation of $\text{Zn}_3(\text{PO}_4)_2$ instead of CePO_4 . For all prepared samples, an absorption band occurred at 430 cm^{-1} due to PO_4 vibration [23].

The IR spectra of the calcinated samples exhibit some difference from the as-prepared samples. This difference depends on the amount of the added zinc cations. In general, the two absorption bands at 3000-3900 and 1630-1650 cm^{-1} disappeared due to the evaporation of the moisture and the water of hydration by heating. For the calcinated samples, a band splitting at the wave number range 1050-950 cm^{-1} was observed. This splitting may be due to the vibration of the PO_4 groups in the phosphates of the monoclinic symmetry [21]. Another splitting at the range of 1200-1090 cm^{-1} appeared at $x = 0.2-1.0$, which is attributed to the formation of $\text{Zn}_2\text{P}_2\text{O}_7$. By following the effects of the addition of zinc content on the IR spectra, two new absorption bands occurred at 760 and 667 cm^{-1} . These bands were attributed to the P-O-P form and the water content as proposed previously by Assaaoudi *et al.* [24]. By raising the zinc content ($x = 0.8-1.0$), a band at 593 cm^{-1} was formed and is attributed to the appearance of the orthophosphates (PO_3 groups). In general, the characteristic bands for the phosphates compound at $\sim 435 \text{ cm}^{-1}$ is observed and continues to appear for all calcinated samples.

For the as-prepared samples with different Zn contents amounts ($x = 0.0-1.0$), the TG/DSC pattern was recorded in

Figure 4. Several sequence weight losses occurred as shown from the recorded patterns. The first weight loss appeared up to $\sim 100 \text{ }^\circ\text{C}$ and is attributed to the loss of physisorbed water which is confirmed by a broad endothermic peak at the same temperature. The second weight loss occurred in the temperature range between 100 to 250 $^\circ\text{C}$ and is attributed to the loss of water of hydration in agreement with the appearance of an endothermic peak on the DSC curve. It is noteworthy that these results confirmed the IR spectrum. By substitution with zinc cations a new weight losses were observed. As the $x = 0.2-0.8$, a weight loss occurred at 300-375 $^\circ\text{C}$ and may be due to the transformation of the CePO_4 from the amorphous state to the crystalline form. The position of this weight loss shifts to lower temperature as the zinc content increases; this may be due to the formation of new compounds as indicated by the X-ray and the IR measurements. At $\sim 600 \text{ }^\circ\text{C}$, a very strong and sharp exothermic band was observed, this may be due to the conversion of the hexagonal phase of CePO_4 to monoclinic or the formation of $\text{Zn}_2\text{P}_2\text{O}_7$ in crystalline structure [25]. At high content of Zn ($x = 1.0$), an endothermic peak was observed at about 375 $^\circ\text{C}$, which may be due to the transformation of ZnHPO_4 to amorphous pyrophosphate by loss of the water content [26]. At 400-525 $^\circ\text{C}$, two weight loss steps occurred and accompanied by two broad exothermic peaks, at the same region caused by the crystalline form of $\text{Zn}_3(\text{PO}_4)_2$ and $\text{Zn}_2\text{P}_2\text{O}_7$, respectively.

The TEM images of the as-prepared and that calcinated at 650 $^\circ\text{C}$ for 2 hrs. are shown in Figure 5. It is observed that at $x = 0.0$, the produced sample is in amorphous one phase. At $x = 0.2$ a very weak crystalline phase embedded into the amorphous was observed as clarified from the corresponding selected area electron diffraction pattern and not detected from the X-ray patterns.

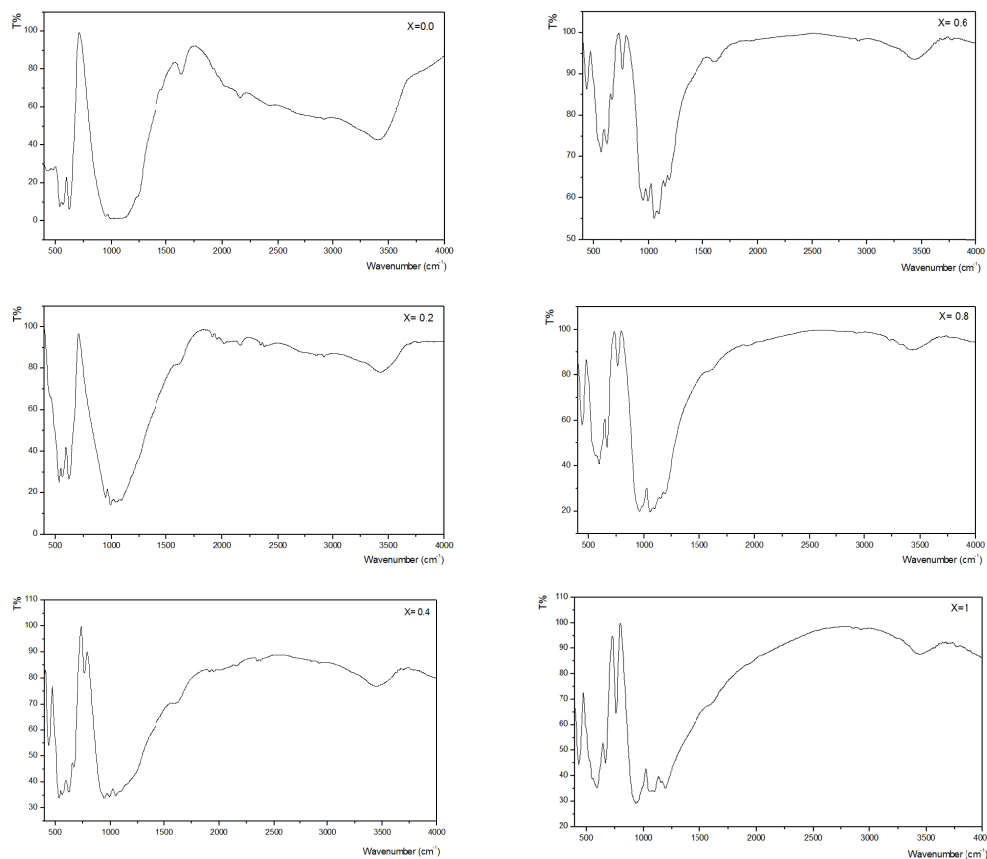


Figure 3. IR spectrum of as prepared and calcined samples zinc phosphate.

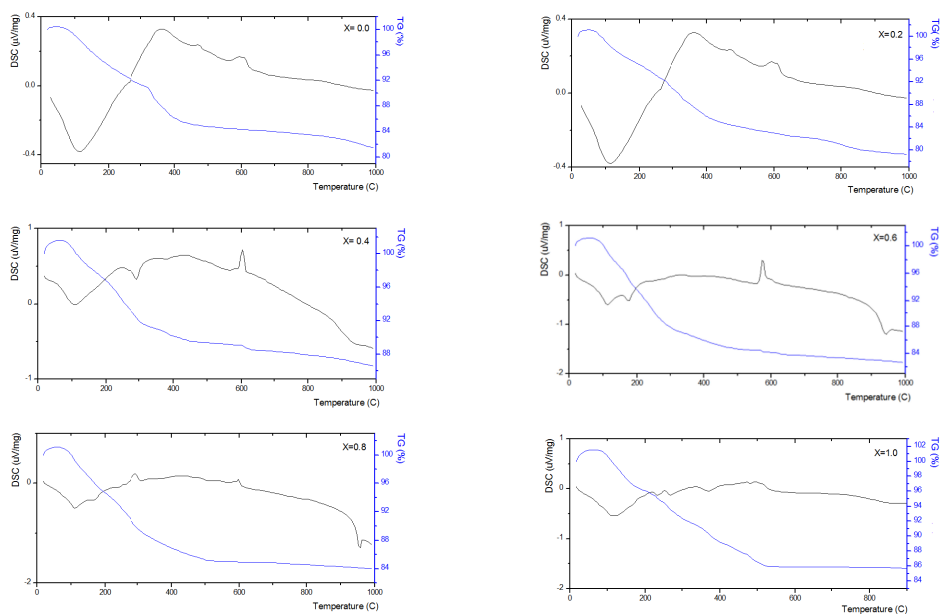


Figure 4. TG and DSC curves of as prepared samples of cerium-zinc phosphate.

As the content of Zn cations increase to 0.6, the same behavior was observed, while by increasing the zinc content to $x = 0.8-1.0$, a high preferred orientation of the crystalline phase in the Z direction was happened.

By calcination at 650 °C for the samples with $x = 0.0-0.2$, the morphology revealed a monoclinic crystalline structure with particle size rang from 20 to 25 nm. At $x = 0.4$, a change in both size and shape of the crystalline structure was observed.

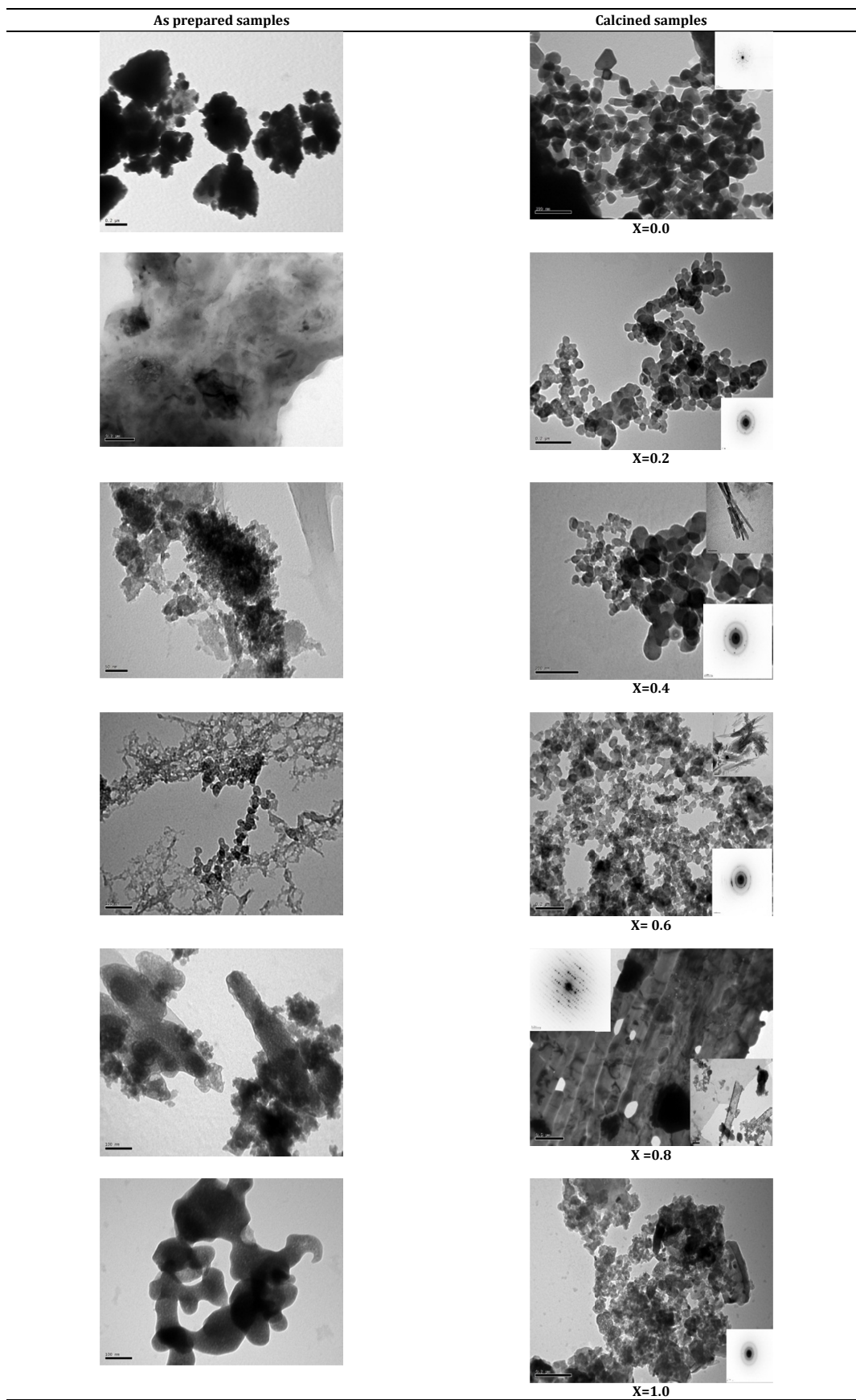


Figure 5. TEM micrographs of as prepared and calcined samples of cerium-zinc phosphate.

In this case a rod like shaped particles and monoclinic crystalline structure with particle size ranging from 30 to 38 nm occurred. The formation of the nano-rods structure may be due to homogen-nucleation. The same behavior was observed for the calcinated samples with $x = 0.6$ and 0.8 with particle size 15 nm where increasing the Zn value will lead to preferred orientation to the crystalline phase which clearly observed from the very fine arrangement of the crystallite phase. It can be seen that the increasing of Zn to Ce improve the crystallinity and the growth tend to be in columnar structure, where the particle size tend to decrease with increasing the zinc ratio to Ce. At $x = 1.0$, the morphology shows a very fine zinc phosphates with particle size ranging from 1 to 8 nm. The effect of the calcination on the morphology of the prepared samples at 650°C is shown in Figure 5.

4. Conclusion

The present work deals with studying the preparation and characterization of the produced phases by replacing Ce cations with Zn cations to be used as shielding agent in the future. A mixtures of Ce-Zn phosphate (with $x = 0.0, 0.2, 0.4, 0.6, 0.8,$ and 1.0) were prepared by reacting $\text{CeSO}_4 \cdot 4\text{H}_2\text{O}$ and $\text{Zn}(\text{CH}_3\text{COO})_2 \cdot 2\text{H}_2\text{O}$ with H_3PO_4 . X-ray results showed an amorphous phase for dried samples occurring at $x = 0.0, 0.2$ and 0.4 . A very weak crystallinity occurred at $x = 0.6$. A complete crystalline form occurred at $x = 0.8$ and 1.0 . For calcined samples, a polycrystalline phases were produced depending on x -value. The thermal analysis TG/DSC indicated that the substitution of Ce^{3+} by Zn^{2+} shifted the crystallization of the produced phases to lower temperatures. The TEM results showed that at $x = 0.4$ - 0.8 for calcined samples; the nano rode structure appeared which has high optical properties. Also TEM indicated that there are high improvements for crystallinity when substituting Ce^{3+} with Zn^{2+} .

Acknowledgments

We appreciate the constructive criticisms by the anonymous reviewers.

References

- [1]. Asano, S. *Hyomenkagaku* **1994**, *15*, 473-476.
- [2]. Masaki, H. *Fragrance J.* **1998**, *26*, 65-69.
- [3]. Neades, R.; Cox, L.; Pelling, J. C. *Mol. Carcinog.* **1998**, *23*, 159-163.
- [4]. Lowe, N. J.; Shaath, N. A.; Pathak, M. A. (Eds), 2 edn., Marcel Dekker, New York, 1997.
- [5]. Reisch, M. S. *Chem. Eng. News.* **2001**, *79*, 25-28.
- [6]. Schlumpf, M.; Berger, L.; Cotton, L. B. Conscience-Egli, M.; Durrer, S.; Fleischmann, I.; Haller, V.; Maerker, K.; Lichtensteiger, W. *Sofw. J.* **2001**, *127*, 10-16.
- [7]. Dransfield, G. P. *Radiat. Prot. Dosim.* **2000**, *91*, 271-273.
- [8]. Yabe, S.; Sato, T. *J. Solid State Chem.* **2003**, *171*, 7-11.
- [9]. Masui, T.; Hirai, H.; Hamada, R.; Imanaka, N.; Adachi, G.; Sakata, T.; Mori, H. *J. Mater. Chem.* **2003**, *13*, 622-627.
- [10]. Fujishima, A.; Honda, K. *Nature* **1972**, *238*, 37-38.
- [11]. Herrmann, J. M.; Guillard, C.; Pichat, P. *Catal. Today* **1993**, *17*, 7-20.
- [12]. Trovarelli, A. *Catalysis by ceria and related materials*, Imperial College Press, London, 2002.
- [13]. Imanaka, N.; Masui, T.; Hirai, H.; Adachi, G. *Chem. Mater.* **2003**, *15*, 2289-2291.
- [14]. Hirai, H.; Masui, T.; Imanaka, N.; Adachi, G. *J. Alloys Compd.* **2004**, *374*, 84-88.
- [15]. Masui, T.; Hirai, H.; Imanaka, N.; Adachi, G. *J. Alloys Compd.* **2006**, *408-412*, 1141-1144.
- [16]. Hanna, A.; Mousa, S. M.; Elkomy, G. M.; Sherief, M. A. *Eur. J. Chem.* **2010**, *1(3)*, 211-215.
- [17]. Patnaik, P. *Inorganic Chemicals*, Mc Graw-Hill, 2002.
- [18]. Bo, L.; Liya, S.; Xiaozhen, L.; Shuiche, Z.; Yumeri, Z.; Tianmain, W.; Sasaki, Y.; Ishii, K.; Kashiwaya, Y.; Takahashi, H.; Shibayama, T. *J. Mater. Sci. Lett.* **2001**, *20*, 1071-1075.
- [19]. Kandori, K.; Yasukawa, A.; Ishikawa, T. *Chem. Mater.* **1995**, *7*, 26-32.
- [20]. Aramendia, M. A.; Borau, V.; Jimenez, C.; Marinas, J. M.; Romero, F. J. *J. Catal.* **1995**, *151*, 44-49.
- [21]. Hazel, A.; Ross, S. D. *Spectrochim. Acta. A* **1966**, *22*, 1949-1961.
- [22]. Pawlig, O.; Trettin, R. *Mater. Res. Bull.* **1999**, *34*, 1959-1966.
- [23]. Aramendia, M. A.; Borau, V.; Jimenez, C.; Marinas, J. M.; Romero, F. J. *J. Colloid Interface Sci.* **1999**, *217*, 288-298.
- [24]. Assaaoudi, H.; Butler, J.; Kozinski, J.; Garipey, F. B. *J. Chem. Crystallogr.* **2005**, *35(1)*, 49-59.
- [25]. Guo, Y.; Woznicki, P.; Barkatt, A. *J. Mater. Res.* **1996**, *11(3)*, 639-648.
- [26]. Sadiq, M.; Bensitel, M.; Lamonier, C.; Leglise, J. *Solid State Sci.* **2008**, *10*, 434-437.